“HARMONIE 37h1 radiation sensitivity tests” Supplement 4: Comparison of running with and without default aerosols

Kristian P. Nielsen [1], Emily Gleeson [2] & Laura Rontu [3]

1. Danish Meteorological Institute, Lyngbyvej 100, DK-2100, Copenhagen Ø, Denmark.
2. Met Éireann, Glasnevin Hill, Dublin 9, Ireland.
3. Finnish Metorological Institute, Erik Palménin Aukio 1, FI-00560 Helsinki, Finland.

In this supplement we show and discuss a comparison between libRadtran/DISORT and HARMONIE calculations, similar to our initially submitted manuscript (Nielsen et al. 2013), but now without aerosol. This comparison was suggested by Referee #2 (Anonymous 2014). In the present comparison, we also use the Kato et al. (1999) transmission functions for DISORT, as suggested by referee #1 (Anonymous 2014). A comparison between libRadtran/DISORT with Kato et. al (1999) functions and HARMONIE, but with aerosol included in both, can be found in a separate supplement.

In Figs. 1–3 and 13–15 the effect on running with aerosols (the left hand side plots) and without aerosols (the right hand side plots) on the clear sky experiments are shown. It is clear that the IFS radiation scheme compares better to the libRadtran/DISORT when the clear sky experiments are run without aerosols. In Fig. 2 it can particularly be seen that the errors at the lower solar zenith angles shown for the IFS radiation scheme relative to DISORT become much less when aerosols are not included. For the solar zenith angle experiment both cases have been run with the pseudo-spherical DISORT solver of Dahlback & Stamnes (1991). Thus, it can be concluded that the differences seen in the left hand side of Fig. 2 and in our initially submitted manuscript (Nielsen et al. 2013) were mostly due to the different aerosol schemes used in libRadtran, IFS and hlradia.

In the cloudy sky experiments shown in Figs. 4–12 and 16–28 significant differences are also seen after rerunning the experiments without aerosols, in particular for the cases with clouds overlying high albedo surfaces (Figs. 7, 8, 10, 12, 15 and 16). In these the IFS simulated global radiation and net fluxes now compare better to the DISORT results. Our new parametrization, IFS (Nielsen), is also seen to compare better to the DISORT results when both HARMONIE and libRadtran are run without aerosols. Overall running without aerosols is a better way to run these experiments, but we do not find that the main conclusions made in the original manuscript (Nielsen et al. 2013) need to be changed.

For further information about the experiments and results presented here please consult the original manuscript (Nielsen et al. 2013) and the references in this. The only change relative to this, is that the experiments have been rerun for the full shortwave spectral range rather than the interval from 280 nm to 3001 nm.

References

[1] Dahlback, A. and Stamnes, K.: A new spherical model for computing the radiation field available for photolysis and heating at twilight, Planet. Space Sci., 39, 671–683, 1991.

[2] Kato, S., Ackerman, T. P., Mather, J. H., and Clothiaux, E.: The k-distribution method and correlated-k approximation for a shortwave radiative transfer model, J. Quant. Spec. Rad. Transfer, 62, 109–121, 1999.

[3] Nielsen, K. P., Gleeson, E. and Rontu L.: Radiation sensitivity tests of the HARMONIE 37h1 NWP model, Geosci. Model Dev. Discuss., 6, 6775-6834, www.geosci-model-dev-discuss.net/6/6775/2013/doi:10.5194/gmdd-6-6775-2013, 2013.

[4] Anonymous referee #1: Review of "Radiation sensitivity tests of the HARMONIE 37h1 NWP model," Geosci. Model Dev. Discuss., 6, C2479C2483, www.geosci-model-dev-discuss.net/6/C2479/2014/, 2014.

[5] Anonymous referee #2: Review of "Radiation sensitivity tests of the HARMONIE 37h1 NWP model," Geosci. Model Dev. Discuss., 6, C2522C2526, www.geosci-model-dev-discuss.net/6/C2522/2014/, 2014.

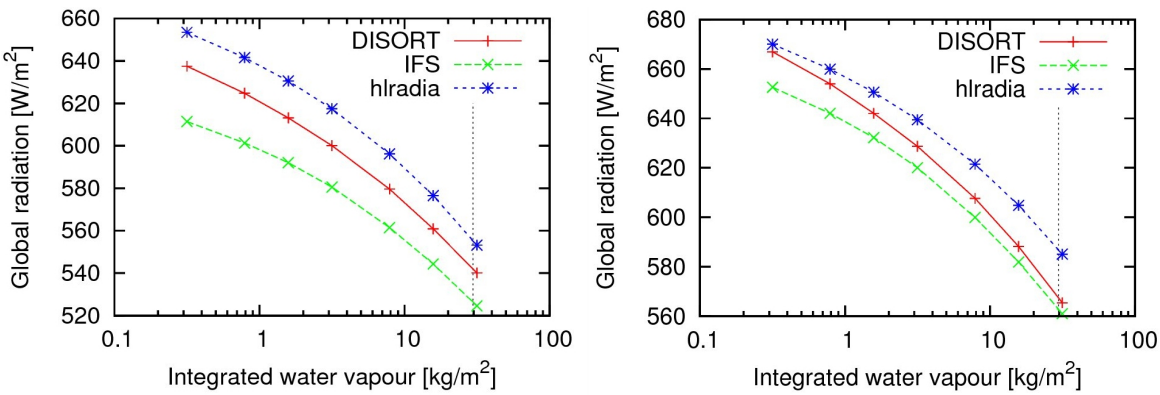

Figure 1: Comparison of global radiation results as a function of integrated atmospheric water vapour. The results from DISORT (red line with +), IFS (green line with x) and hlradia (blue line with *) are shown. The vertical dashed line marks the reference integrated water vapour used in the other experiments. **Left:** The results for the case where default aerosols are included in all models. **Right:** The results for the case where aerosols are removed from all models.

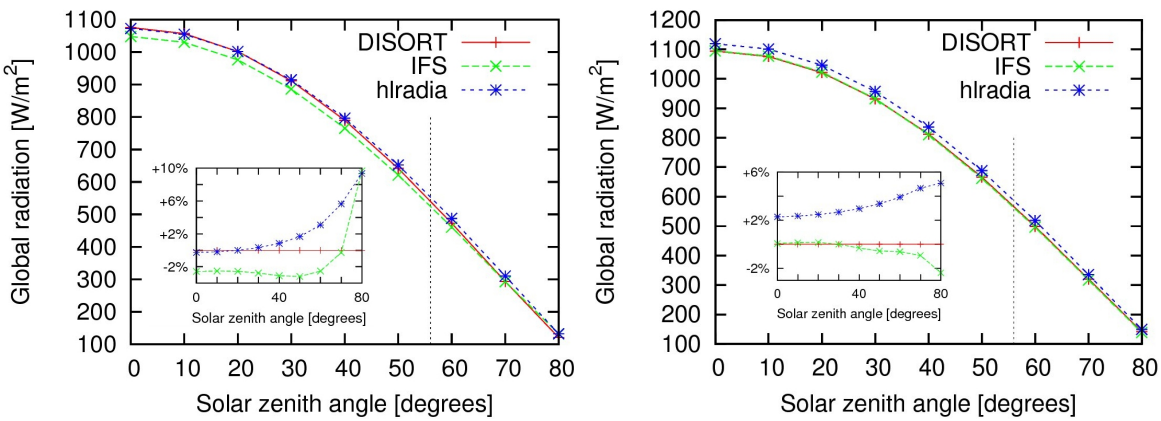

Figure 2: As for Fig. 1 but for a varying solar zenith angle. The subplots show the corresponding relative differences defined as (X-DISORT)/DISORT·100%.

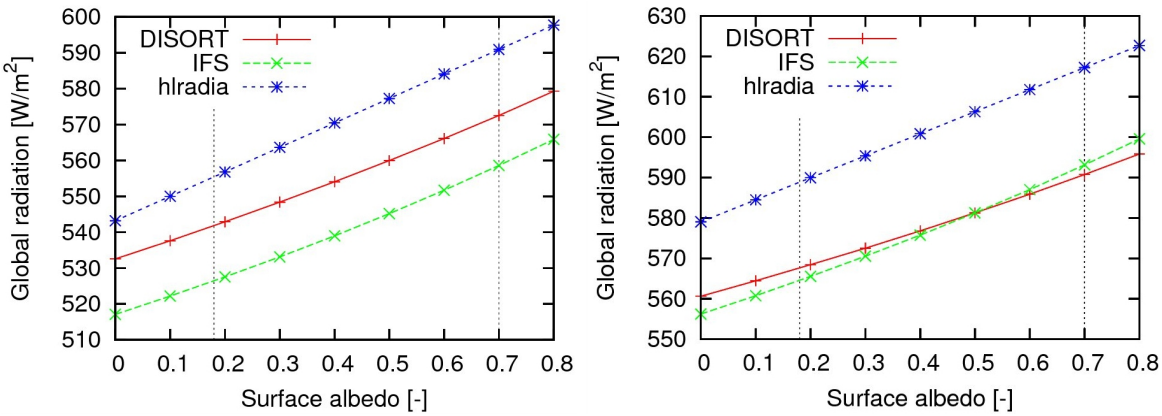

Figure 3: As for Fig. 1 but for a varying surface albedo in clear sky conditions.

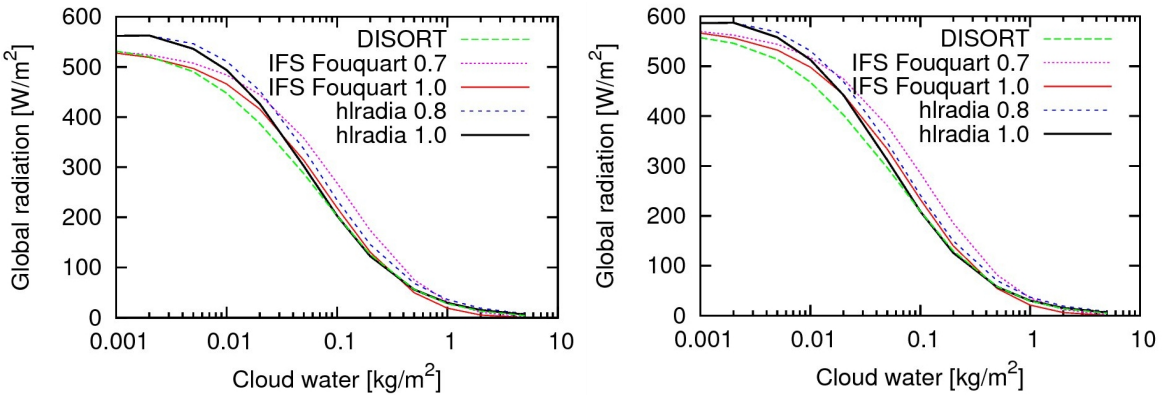

Figure 4: Comparison of global radiation results as a function of integrated liquid cloud water. The results from DISORT (green dashed curve), IFS Fouquart with SW inhomogeneity factors of 0.7 (magenta dotted curve) and 1.0 (red curve), and hlradia with SW inhomogeneity factors of 0.8 (blue dashed curve) and 1.0 (black curve) are shown. **Left:** The results for the case where default aerosols are included in all models. **Right:** The results for the case where aerosols are removed from all models.

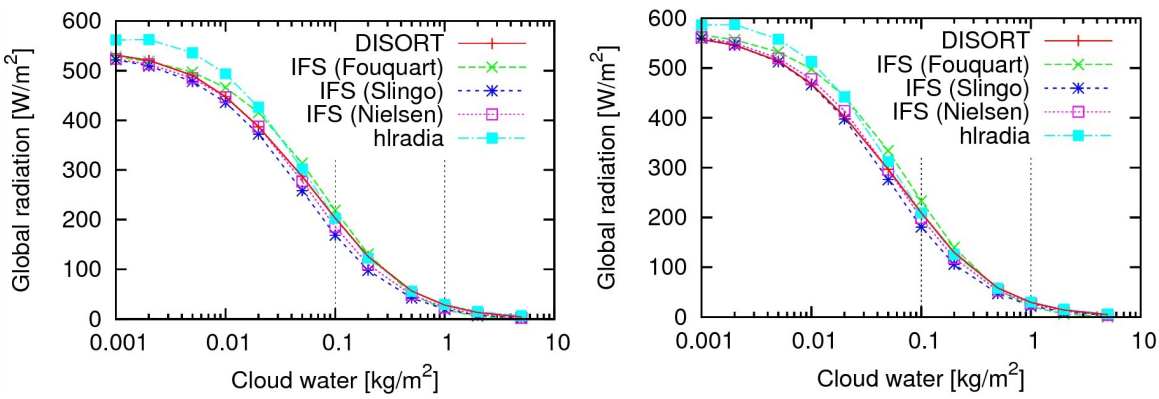

Figure 5: As for Fig. 4 but here the SW inhomogeneity factor is 1.0 in all cases. The results for DISORT (red curve with +s), IFS Fouquart (green curve with xs), IFS Slingo (blue curve with *s), IFS Nielsen (magenta curve with boxes) and hlradia (cyan curve with filled boxes) are shown.

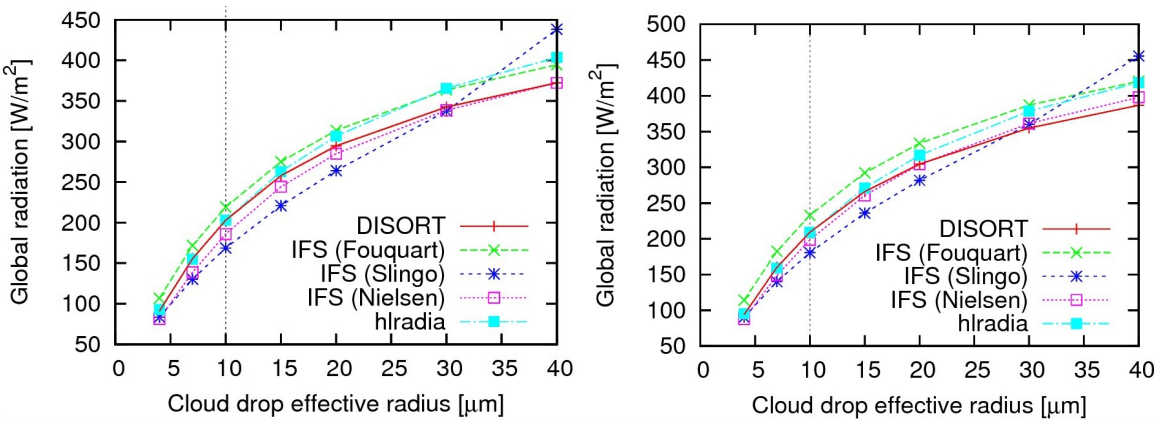

Figure 6: As for Fig. 5 but for a varying cloud drop effective radius.

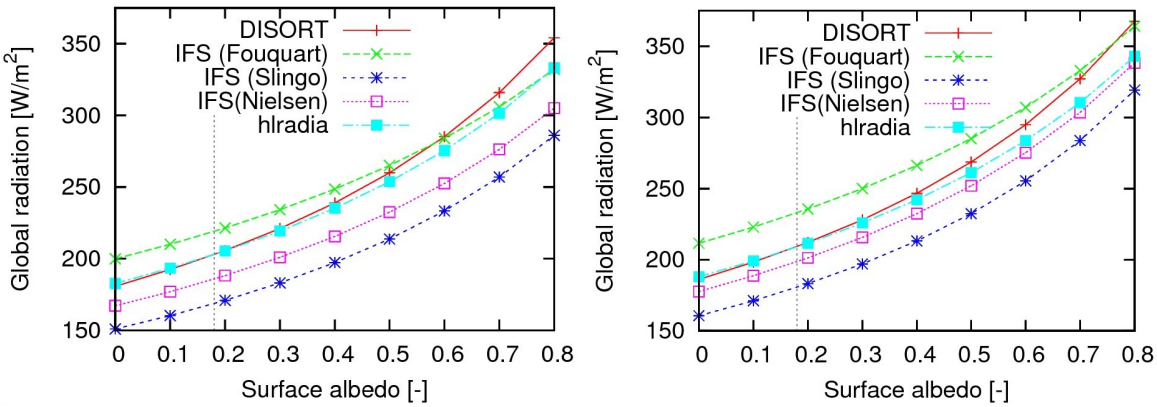

Figure 7: As for Fig. 5 but for a varying surface albedo under a cloud with 0.1 kg/m^2 cloud liquid water.

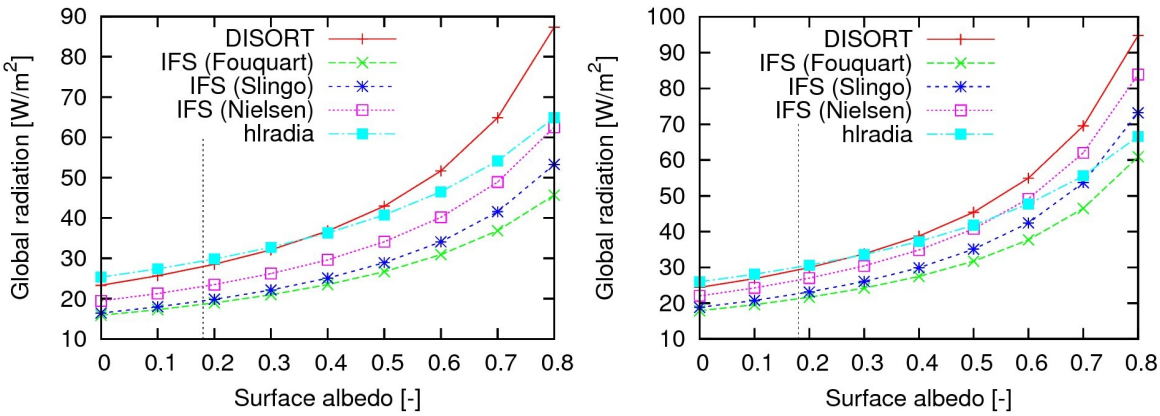

Figure 8: As for Fig. 5 but for a varying surface albedo under a cloud with 1.0 kg/m^2 cloud liquid water.

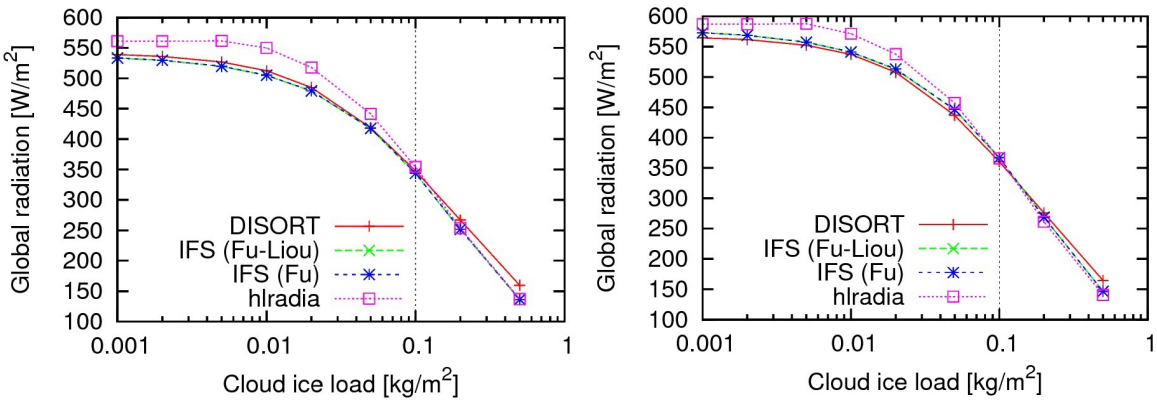

Figure 9: As for Fig. 5 but for a varying cloud ice load.

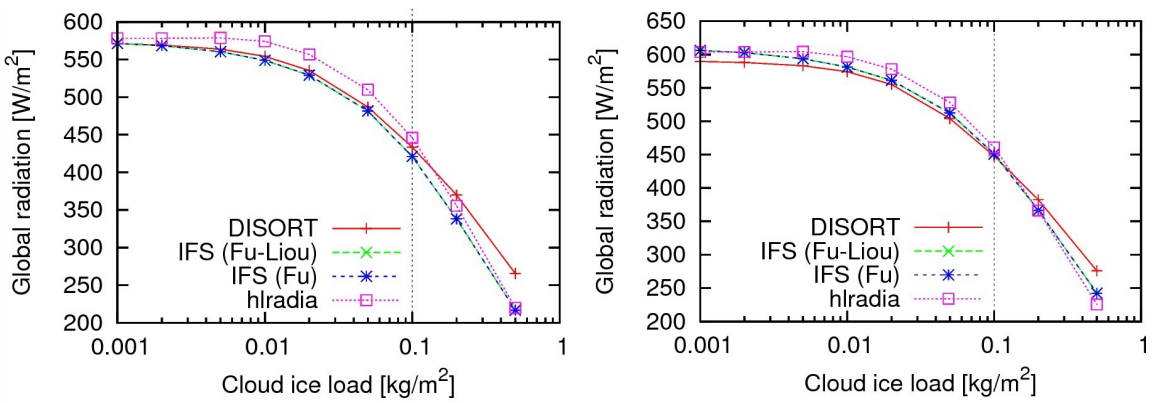

Figure 10: As for Fig. 9 but for surface albedo = 0.7.

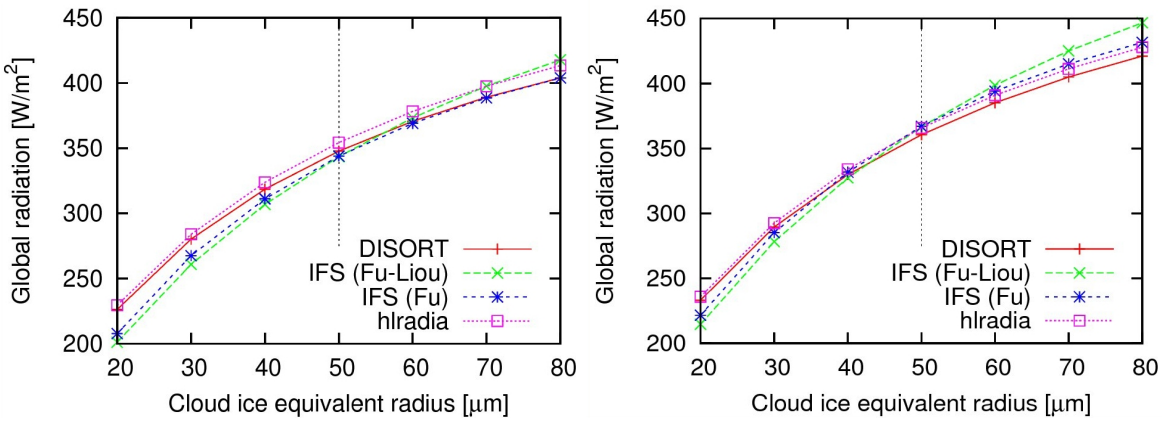

Figure 11: As for Fig. 5 but for a varying cloud ice equivalent radius.

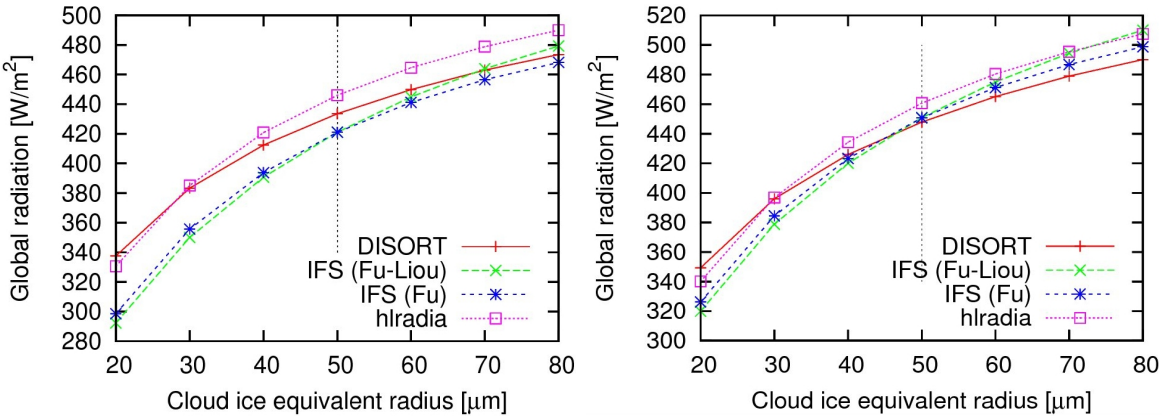

Figure 12: As for Fig. 11 but for surface albedo = 0.7.

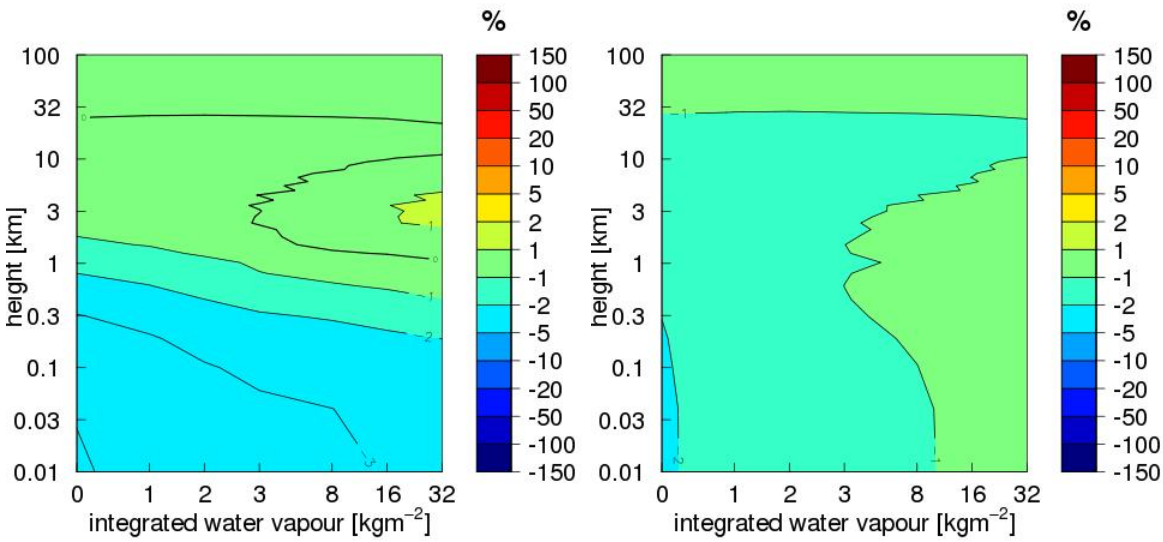

Figure 13: Relative differences (%) in net fluxes between the IFS radiation scheme and DISORT shown as a function of integrated water vapour and height.

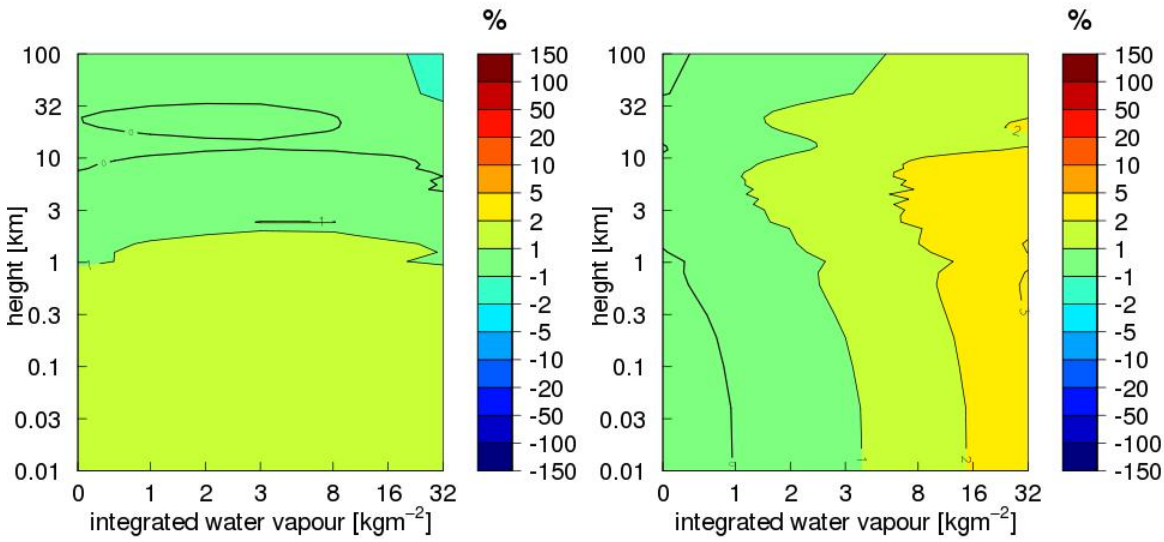

Figure 14: As for Fig. 13 but for hlradia compared to DISORT.

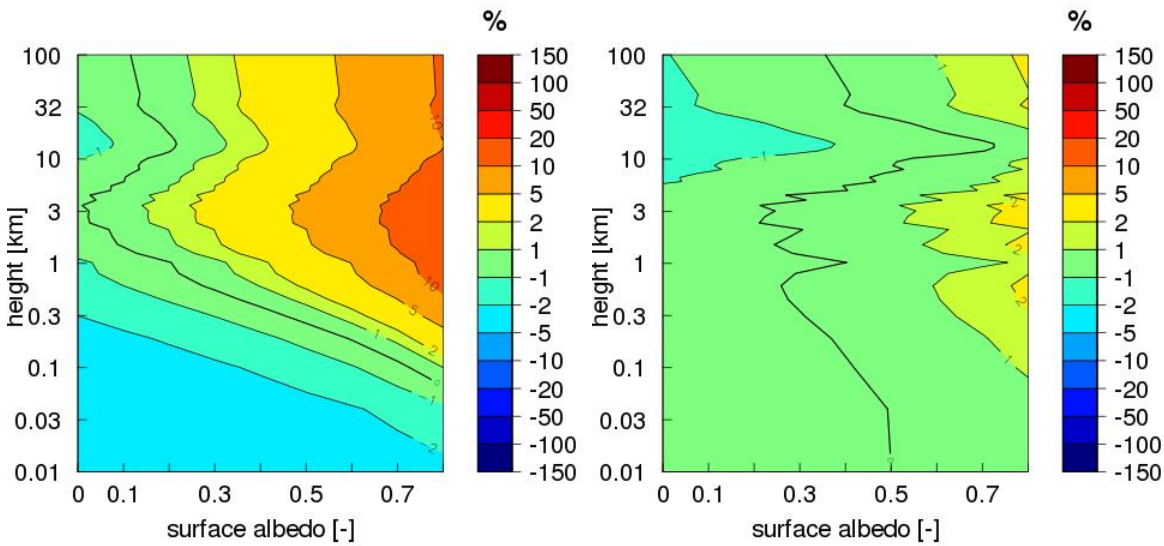

Figure 15: As for Fig. 13 but for IFS vs DISORT as a function of surface albedo.

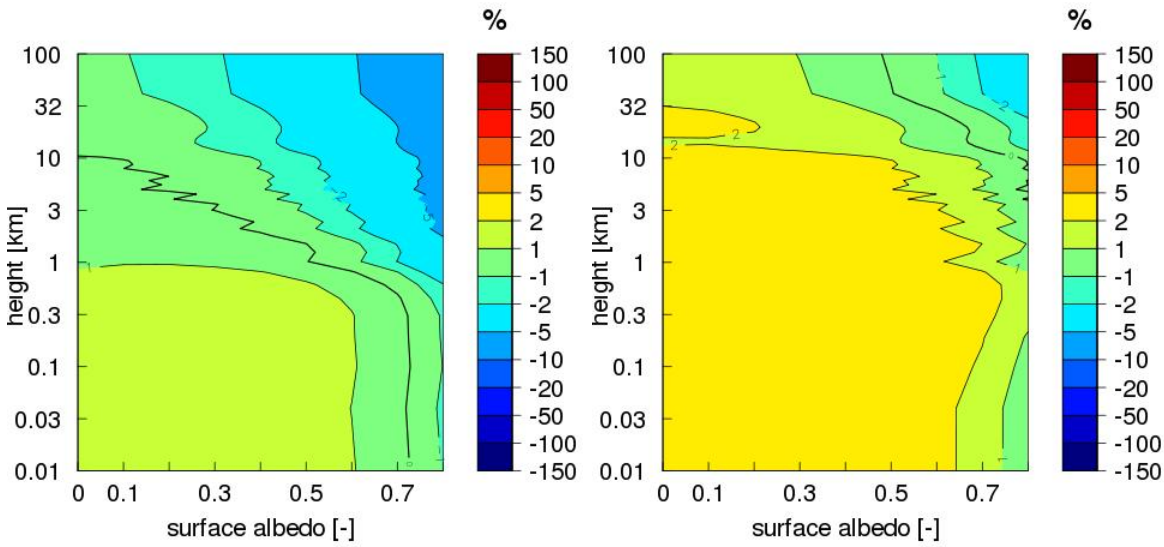

Figure 16: As for Fig. 15 but for hlradia compared to DISORT.

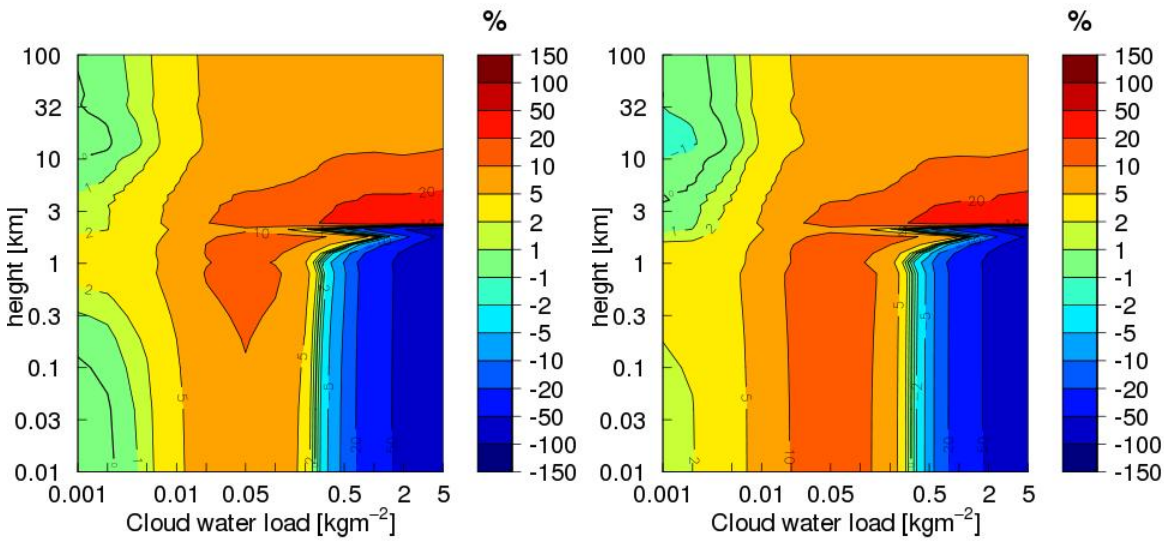

Figure 17: As for Fig. 13 but for cloud water load and IFS-Fouquart vs DISORT

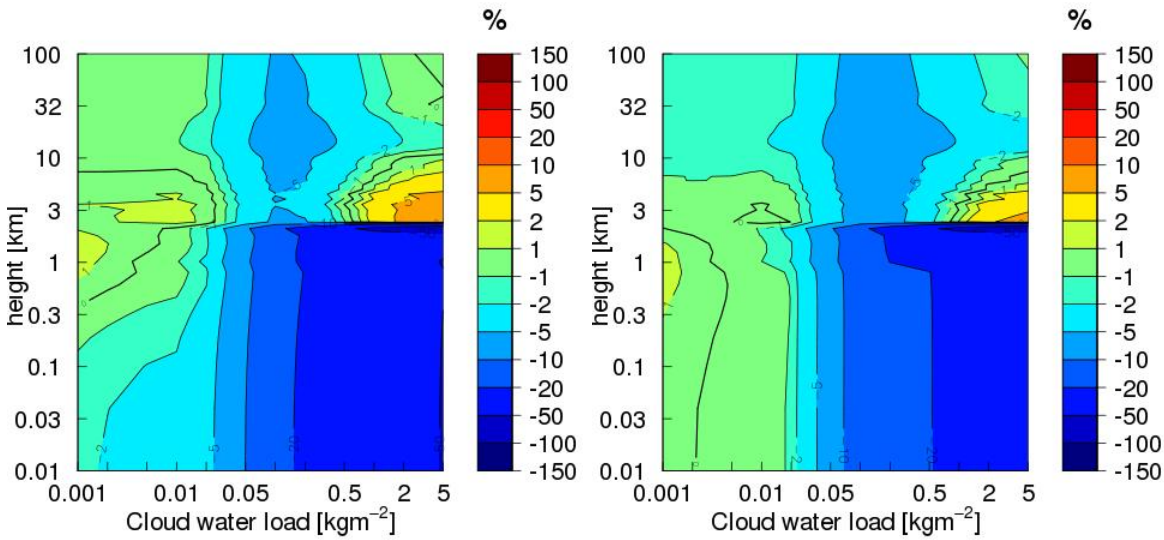

Figure 18: As for Fig. 17 but for IFS-Slingo vs DISORT.

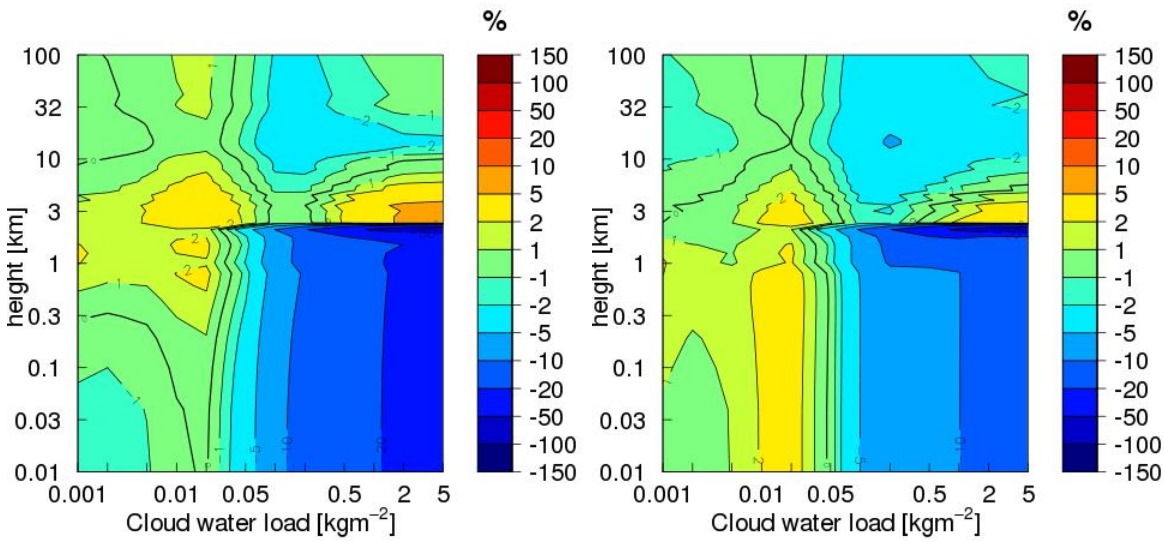

Figure 19: As for Fig. 17 but for IFS-Nielsen vs DISORT.

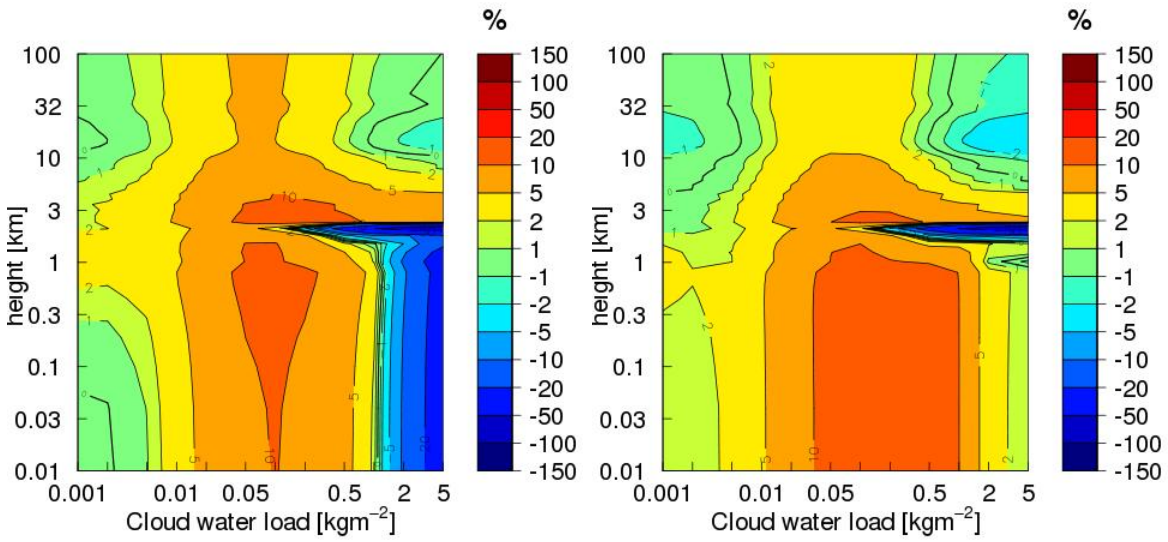

Figure 20: As for Fig. 19 but for IFS-Nielsen with the Hopf q-function set to 0.71 vs DISORT.

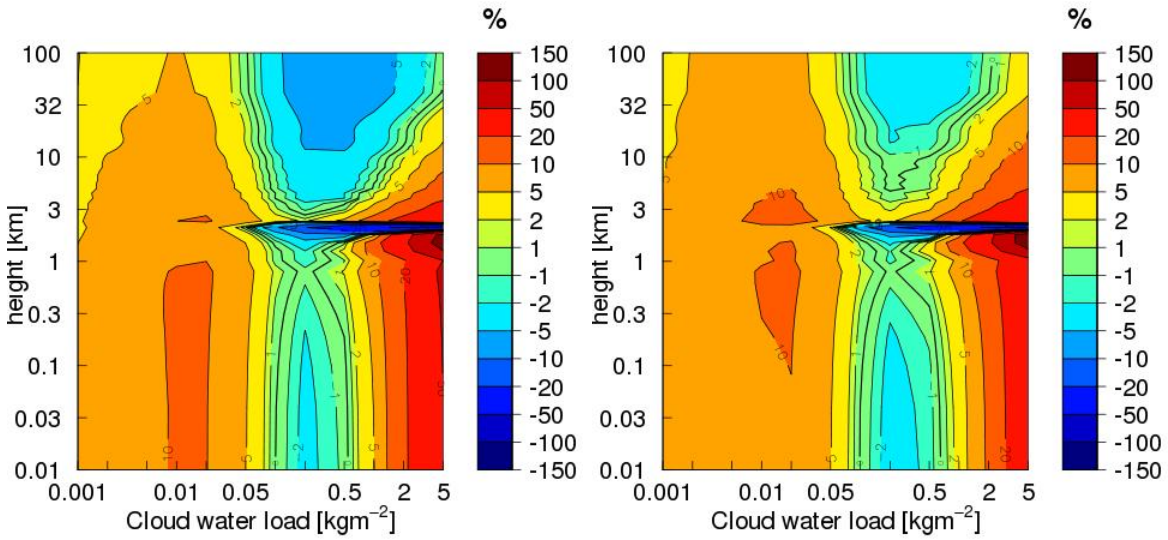

Figure 21: As for Fig. 17 but for hlradia vs DISORT.

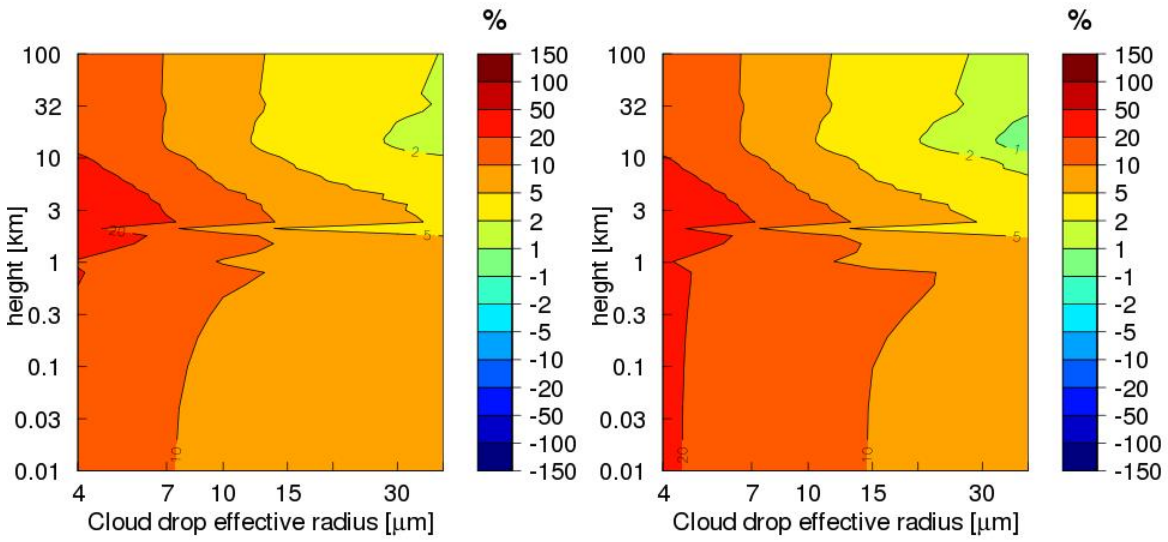

Figure 22: As for Fig. 13 but for cloud drop effective radius and IFS-Fouquart vs DISORT

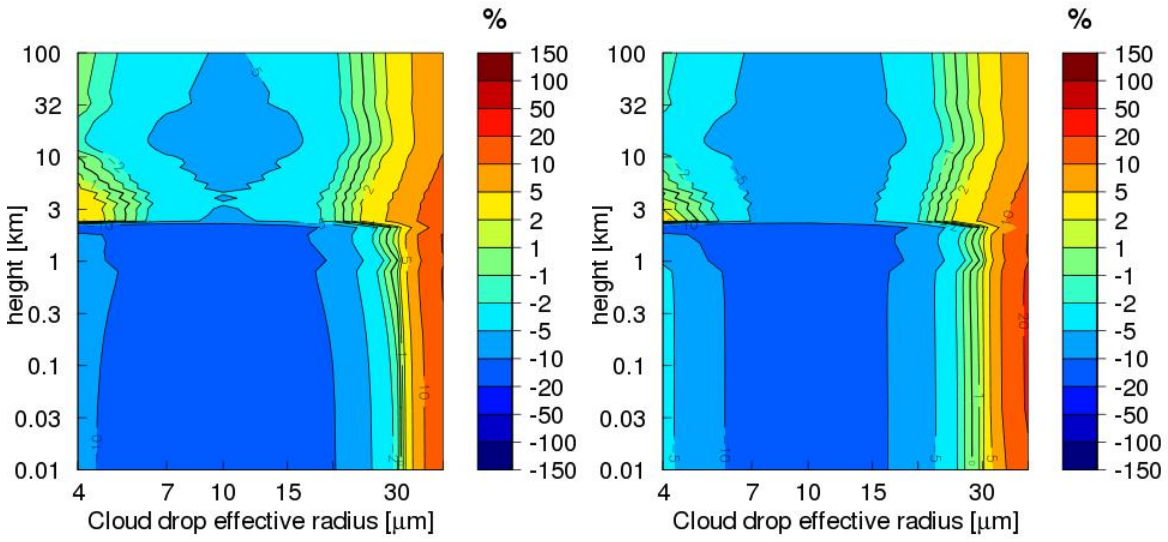

Figure 23: As for Fig. 22 but for IFS-Slingo vs DISORT.

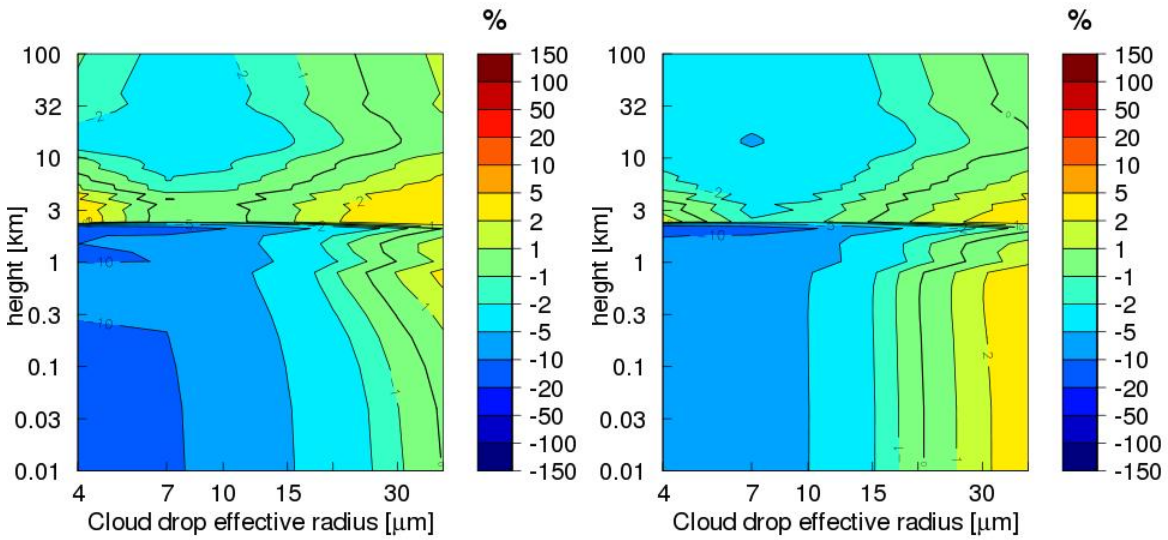

Figure 24: As for Fig. 22 but for IFS-Nielsen vs DISORT.

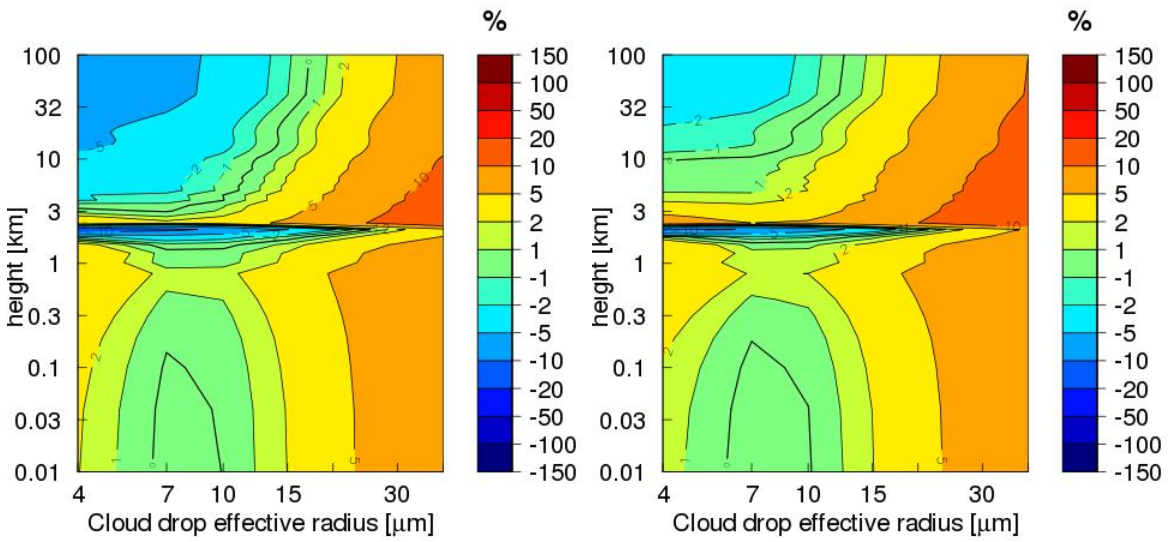

Figure 25: As for Fig. 22 but for hlradia vs DISORT.

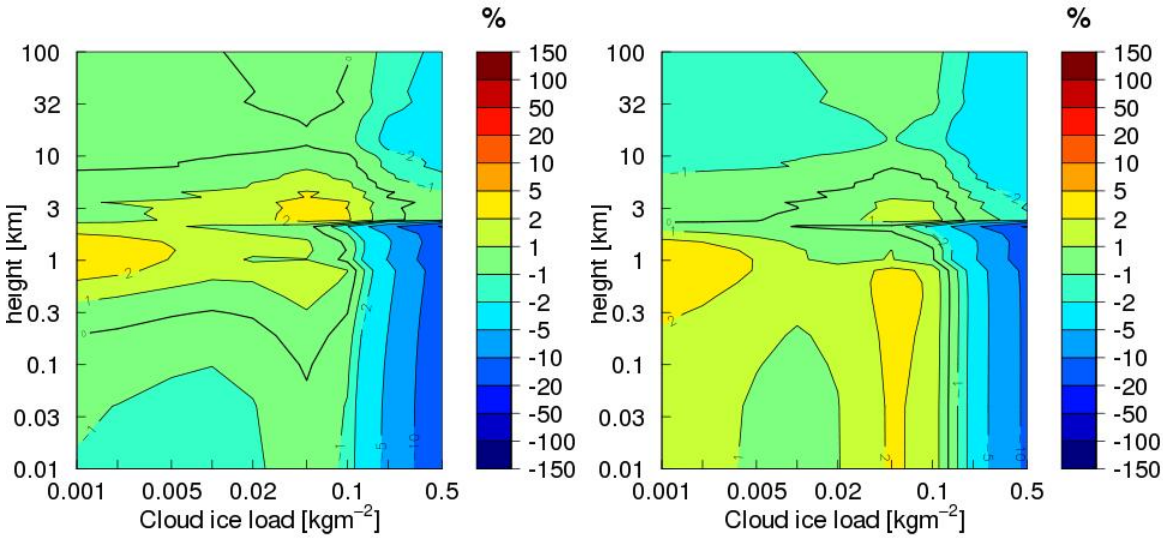

Figure 26: As for Fig. 13 but for cloud ice load and the IFS radiation scheme using the Fu and Liou (1993) ice cloud optical property parametrization vs DISORT.

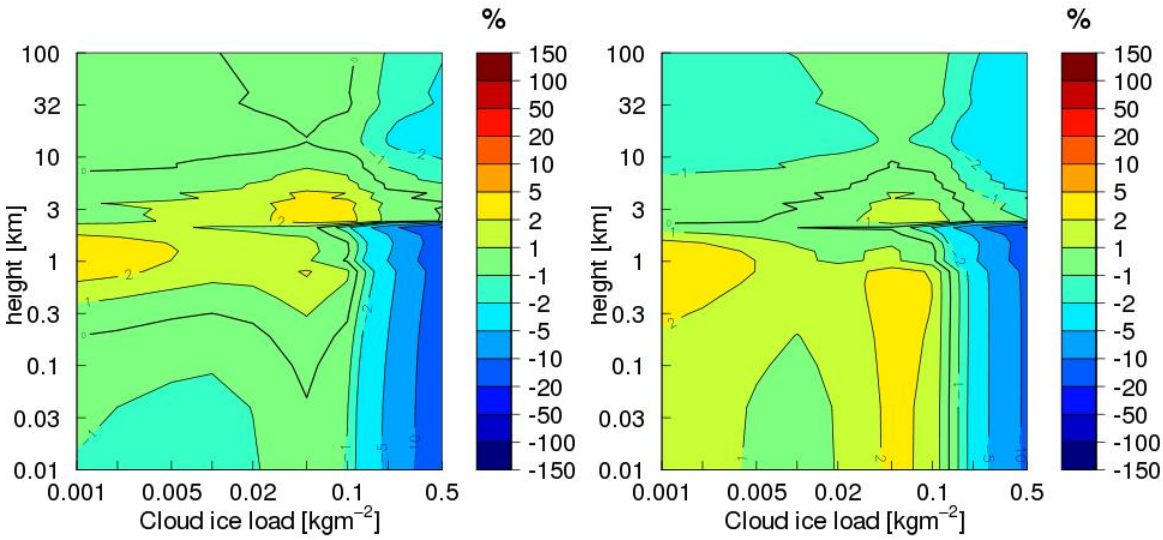

Figure 27: As for Fig. 26 but for IFS with the Fu (1996) ice cloud optical property scheme vs DISORT.

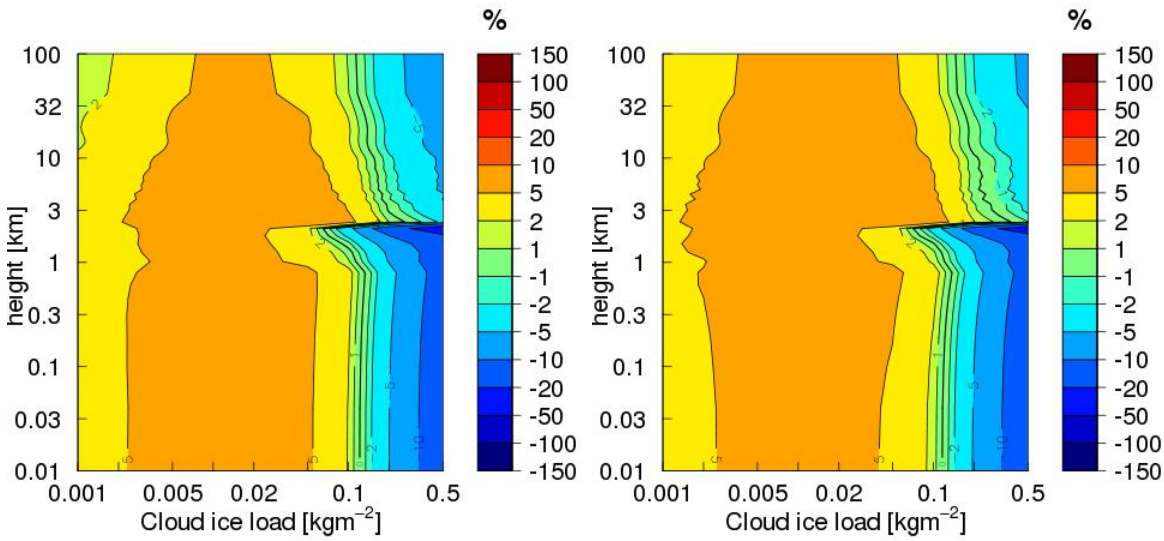

Figure 28: As for Fig. 26 but for hlradia vs DISORT.